International Journal of Chemical, Material and Environmental Research 2015, 2 (3): 1-16

Research article

INTERNATIONAL JOURNAL OF CHEMICAL, MATERIAL AND ENVIRONMENTAL RESEARCH

An International Open Free Access, Peer Reviewed Research Journal

ISSN 2410-5945
2015, Vol. 2, No. 3:
pg. 1-16

Quantum Chemical Studies on the Corrosion Inhibitions of Mild Steel in Acidic Medium by 5-amino-1-cyclopropyl-7-[(3R,5S)-3,5-dimethylpiperazin-1-yl]-6,8-difluoro-4-oxo-1,4-dihydroquinoline-3-carboxylic acid

Paul Ocheje Ameh*, Sholadoye Q. Oyeniyi, Umar M. Sani

Department of Chemistry, Nigeria Police Academy, Wudil, Kano, Nigeria

(Received: April 27, 2015; Accepted: May 26, 2015)

Abstract

Experimental aspect of the corrosion inhibition of mild steel in phosphoric acid by 5-amino-1-cyclopropyl-7-[(3R,5S)-3,5-dimethylpiperazin-1-yl]-6,8-difluoro-4-oxo-1,4-dihydroquinoline-3-carboxylic acid (ACA) was carried out using gravimetric, gasometric and thermometric methods while theoretical studies were carried out using quantum chemical and density functional theory (DFT) approaches. The results obtained indicated that ACA is a good adsorption inhibitor for the corrosion of mild steel in H_3PO_4 solutions. The adsorption of the inhibitor on mild steel surface was found to be spontaneous and was described by Temkin adsorption model. From the values of free energy of adsorption, a physical adsorption mechanism has been proposed for the adsorption. The average inhibition efficiencies correlated strongly with some quantum chemical parameters (frontier molecular orbital energies, energy gap, electronic energy of the molecule, core - core repulsion energy, dipole moment, and heat of formation) calculated. The adsorption of ACA on the metal surface would preferentially be through the N (20), O (12) and O (14).

Keywords: Acid, corrosion inhibitors, quantum chemical calculations, adsorption, Fukui function, mild steel

1. Introduction

Due to its mechanical properties, mild steel is used in the construction of numerous industrial equipment and appliances [1, 2], however, its life span when in contact with acidic medium over a period depends on the protection or inhibition techniques adopted in such an environment. Several inhibitors have been synthesized and used for this purpose [3-6]. Generally, an inhibitor is a compound that is normally added in small amount in order to slow down the rate of corrosion [7, 8]. Most efficient inhibitors are organic compounds containing electronegative functional groups and π-electrons in triple or conjugated double bonds. Heteroatoms such as sulphur, phosphorus, nitrogen and oxygen as well as aromatic rings are the major adsorption centers of these compounds [9, 10]. The compounds function as inhibitors for metals by virtue of adsorption on the metal surface, blocking the active sites and thereby decreasing the corrosion rate [11]. They control corrosion by acting over the anodic or the cathodic surface or both.

Quantum chemical methods have already proven to be very useful in determining the molecular structure as well as pro-

* Corresponding author:
nocaseoche@yahoo.com
Published online at www.ijcmer.org
Copyright © 2015 Int. J. Chem. Mater. Environ. Res. All Rights Reserved.

viding detailed information on the electronic structure and reactivity of chemical compounds [12]. Thus, it has become a common practice to carry out quantum chemical calculations in corrosion inhibition studies. Recently, theoretical prediction on the efficiency of corrosion inhibitors has become very popular in parallel with the progress in computational hardware and the development of efficient algorithms [13, 14]. This has assisted the routine development of molecular quantum mechanical calculations. In view of the numerous advantages offered by quantum chemical parameters, some studies have been carried out on corrosion inhibition processes using quantum chemical parameters or descriptors [4, 5, 6, 15-17].

The objective of this study is to investigate the inhibition potentials of 5-amino-1-cyclopropyl-7-[(3R,5S)-3,5-dimethylpiperazin-1-yl]-6,8-difluoro-4-oxo-1,4-dihydroquinoline-3-carboxylic acid [ACA] (Figure 1) in hydrochloric acid using experimental and theoretical techniques.

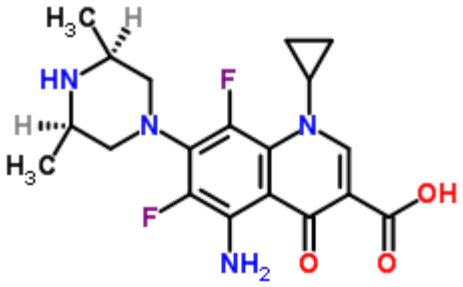

Figure 1. Chemical Structure of 5-amino-1-cyclopropyl-7-[(3R,5S)-3,5-dimethylpiperazin-1-yl]-6,8-difluoro-4-oxo-1,4-dihydroquinoline-3-carboxylic acid

The experimental aspect of the study was carried out using gravimetric, gasometric and thermometric methods while the theoretical calculations were semi-empirical, ab initio methods, density functional theory (DFT) and Fukui function analysis. Calculations were performed with the aid of Chem Office Ultra 2013, MOPAC 7.0, Hyperchem 8.0 release, Chem Pro and Materials Studio softwares. Substituent constants, quantum chemical descriptors and local selectivity indices were then used to predict the inhibition potentials of the studied carboxylic acid.

2. Materials and Methods

2.1. Weight Loss

A previously weighed metal (mild steel) coupon was completely immersed in 250 mL of the test solution in an open beaker. The beaker was covered with aluminium foil and inserted into a water bath maintained at 303 K. After every 24 h, the corrosion product was removed by washing each coupon (withdrawn from the test solution) in a solution containing 50% NaOH and 100 g/L of zinc dust. The washed coupon was rinsed in acetone and dried in the air before re-weighing. The procedure was repeated at 313, 323 and 333 K. In each case, the weight of the sample before immersion was measured using Scaltec high precision balance (Model SPB 31).The difference in weight for a period of 168 h was taken as total weight loss. The inhibition efficiency (% I) for each inhibitor was calculated using the formula expressed in Equation 1.

$$\%I = \left(1 - \frac{W_1}{W_2}\right) \times 100 \qquad 1$$

where W_1 and W_2 are the respective weight losses (g/L) for mild steel in the presence and absence of inhibitor in H_3PO_4 solution. The degree of surface coverage (θ) is given by Equation 2.

$$\theta = \left(1 - \frac{W_1}{W_2}\right) \qquad 2$$

The rates for mild steel corrosion in different acid concentrations and other media have been determined for 168 h immersion period from weight loss using Equation 3 [18].

$$Corrosion\ \ rate = 534W / DAT \qquad 3$$

where *W* is the weight loss of the specimen (mg); *D* is the density of specimen (g/mL), *A* is the area of specimen (square inches) and *T* is the period of immersion (h).

2.2. Synergistic Study

Synergistic study was carried out using weight loss. However, each concentration of the test solution was mixed with 0.06 M of the respective halides (namely, KBr, KI and KCl), from the calculated inhibition efficiencies, synergistic parameters were obtained using Equation 4.

$$S = \frac{1-\eta_A+\eta_A\eta_B}{1-\eta_{AB}} \quad 4$$

where η_A and η_B are inhibition efficiencies of compounds A and B, respectively. η_{AB} is the inhibition efficiency of a combination of the two inhibitors.

2.3. Gasometry Method

The gasometric measurement was carried out as previously described elsewhere [19] using a gasometric assembly. The progress of corrosion reaction was monitored by careful measurement of the volume of hydrogen gas evolved at fixed time intervals. From this, the corrosion rate (CR) was determined using the expression:

$$\%IE = \frac{V_b - V_t}{V_b} x100 \quad 5$$

where V_b is the volume of hydrogen gas evolved by the blank and V_t is the volume of hydrogen gas evolved in the presence of the inhibitor, after time, *t*.

2.4. Thermometric Method

Thermometric measurements were carried out as reported elsewhere [19]. The reaction number (RN) of each system was calculated by dividing the difference between the highest and lowest temperature attained by the time interval. From RN, the inhibition efficiency (% I) of the inhibitor was calculated using Equation 6.

$$\%I = \frac{RN_{aq} - RN_{wi}}{RN} X100 \quad 6$$

where RN_{aq} and RN_{wi} are the RN in the absence of inhibitors (blank solution) and of 0.1 M H_3PO_4 containing the studied inhibitor, respectively.

2.5. Quantum Chemical Study

Quantum chemical calculations were carried out using PM6, PM3, AM1, RM1, and MNDO semi-empirical (SCF-MO) methods in the MOPAC 7.0 package [6]. Calculations were performed on an HP compatible Pentium V (2.0 GHz and 4GB RAM) computer. The following quantum chemical indices were calculated: the energy of the highest occupied molecular orbital (E_{HOMO}), the energy of the lowest unoccupied molecular orbital (E_{LUMO}), the dipole moment (μ), the total energy (*TE*) and ionization potential (IP). Ab initio parameters (the total charge of the molecules, electron density and Muliken charge on the atom) were computed using the MP2 and B3LYP-6-31G** models in the GAMES programme [5, 6]. Statistical analyses were performed using SPSS program version 15.0 for Windows, while all structures were drawn and optimised using Chem Office Ultra 2013 version.

3. Results and Discussions

3.1. Experimental Study

3.1.1. Corrosion Rate and Inhibition Efficiency

Figure 2 shows the variation of weight loss with time for the corrosion of mild steel in 0.1 M H_3PO_4 containing various concentrations ACA. It is observed from the figure that the extent of weight loss decreased with temperature, as the corrosion inhibition strengthened, with increase in inhibitor concentration. This trend may result from the fact that surface cov-

erage increases with the increase in concentration.

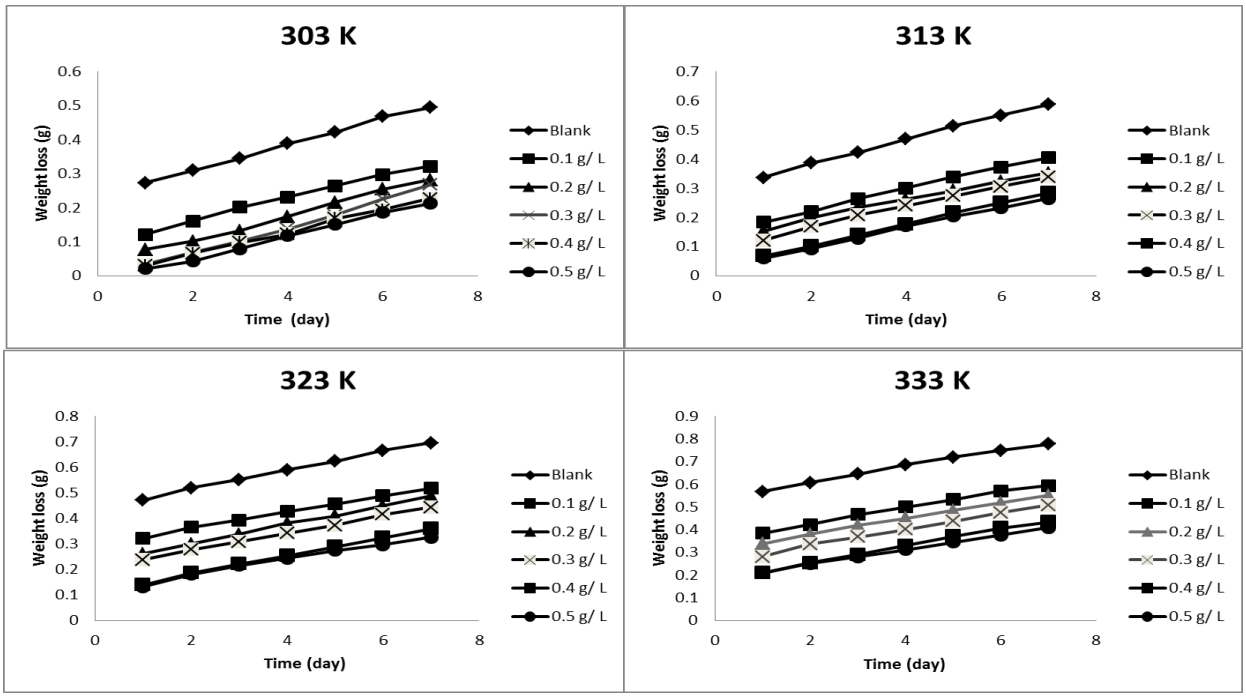

Figure 2. Variation of Weight Loss with Time for the Corrosion of Mild Steel in 0.1 M H_3PO_4 Containing Various Concentrations of ACA at 303, 313, 323 and 333 K

The inhibition efficiency of the ACA on the corrosion of the mild steel in 0.1 M H_3PO_4 containing different concentrations of the ACA is presented in Table 1. The results generally revealed that the inhibition efficiency of mild steel in the various systems increases with increase in concentration but decrease with temperature, indicating that this inhibitor retards the corrosion of mild steel through physical adsorption. This result is consistent with the findings of Martinez [20], Abiola *et al.* [21] and Ameer [22]. The results obtained from thermometric and gasometric experiments (Table 1) show trend similar to those obtained from weight loss experiment (R^2 = 0.9485 and 0.9256 for inhibition efficiency obtained from thermometric and gasometric methods, respectively). The higher values of inhibition efficiencies obtained from later measurements indicate that the instantaneous inhibition efficiencies of ACA are higher than their average inhibition efficiencies. The extent of weight loss essentially indicates inhibition efficiency over an average period of time while thermometric and gasometric signifies inhibition efficiency over a short period of time, usually an hour.

The values of the degree of surface coverage (θ) calculated using Equation 2 are also given in Table 1. The results show trend similar to those of inhibition efficiencies obtained in the study because this property is directly proportional to the inhibition efficiency.

Table 1. Degree of Surface Coverage and Inhibition Efficiency of Various Concentrations of ACA for the Corrosion of Mild Steel in 0.1M H_3PO_4

T (K)	**303**		**313**		**323**		**333**		**Thermometric**	**Gasometric**
C (g/ L)	% I	θ	% I	θ	% I	θ	% I	θ	% I	% I
0.1	55.00	0.5500	50.08	0.5008	44.35	0.4435	42.58	0.4258	67.29	70.00
0.2	64.61	0.6461	61.11	0.6111	51.23	0.5123	47.46	0.4746	73.10	75.30
0.3	67.20	0.6720	64.33	0.6433	57.69	0.5769	54.48	0.5448	77.84	78.25
0.4	76.27	0.7627	70.00	0.7000	67.35	0.6735	63.00	0.6300	81.46	84.02
0.5	79.00	0.7900	75.45	0.7545	74.38	0.7438	67.55	0.6755	86.55	88.90

Figure 3 illustrates the variation of the corrosion rates of the mild steel in 0.1 M H_3PO_4 with inhibitor concentration for an exposure time of 168 h. It can be clearly deduced from the figure that the inhibitor retards the corrosion rate of the mild steel in the test solutions (corrosion rate decreases with increase in inhibitor concentration).

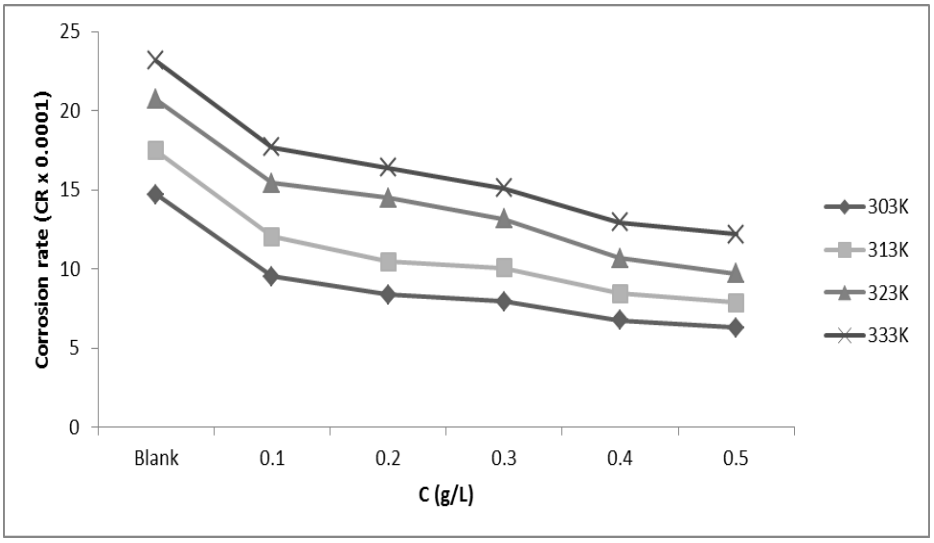

Figure 3. Variation of Corrosion Rate of Mild Steel with Concentration in Solutions of H_3PO_4 Containing Various Concentrations of ACA at 303, 313, 323 and 333 K

3.1.2. Synergistic Studies

Synergistic study was carried out in order to improve the inhibition efficiencies of ACA where various concentrations of inhibitor (0.01-0.05 g/L) was combined with 0.06 M KCl, KBr or KI, respectively. The obtained results (Table 2) showed that the halide ions appear to improve the efficiency of the inhibitor at all concentrations. The addition of the iodide ions was observed to give the highest enhancement. This may be due to their large sizes (Cl = 0.09 nm, Br = 0.114 nm, I = 0.135 nm) and ease of polarizability which is more predisposed to adsorption on metal surfaces and as a consequence exert the highest effect compared to chloride and bromide ions.

The calculated synergistic parameters obtained using Equations 3 are also presented in Table 2. It was observed that all the values are more than unity and this suggests that the enhanced inhibition efficiency caused by the addition of halide ions to the studied inhibitor is in the order $Cl^- < Br^- < I^-$ This could only be attributed to synergistic effect which is consistent with reports made by other researchers [23-25].

Table 2. Inhibition Efficiencies and Synergistic Parameters (S) of ACA in Combination with 0.06 M KI, KBr and KCl.

C (g/L)	Inhibition efficiency			Synergistic parameter (S)		
	KBr + ACA	KI + ACA	KCl + ACA	KBr + ACA	KI + ACA	KCl + ACA
0.01	69.22	75.10	67.23	1.81	1.74	1.83
0.02	74.55	82.44	73.66	1.88	1.79	1.89
0.03	79.66	88.28	78.38	1.85	1.77	1.87
0.04	85.00	93.47	83.90	1.91	1.82	1.92
0.05	92.21	95.56	90.60	1.85	1.84	1.88

3.1.3. Kinetic Study

Kinetic study of the corrosion of mild steel in the presence of different concentrations of ACA was carried out by fitting data obtained from weight loss measurements into different kinetics equations. The test indicated that the corrosion of mild steel in solutions of H_3PO_4 followed first order kinetics, expressed in Equation 7.

$$-\log(weight\ loss) = k_1 t / 2.303 \quad 7$$

where k_1 is the first order rate constant and t is the period of contact. Figure 4 presents the variation of –log (weight loss) versus time for the corrosion of mild steel in H_3PO_4 solution containing ACA. The kinetic parameters deduced from the plots are presented in Table 3. The obtained results indicate that the rate constants decrease with increasing concentration of the respective inhibitor but decrease with increasing temperature.

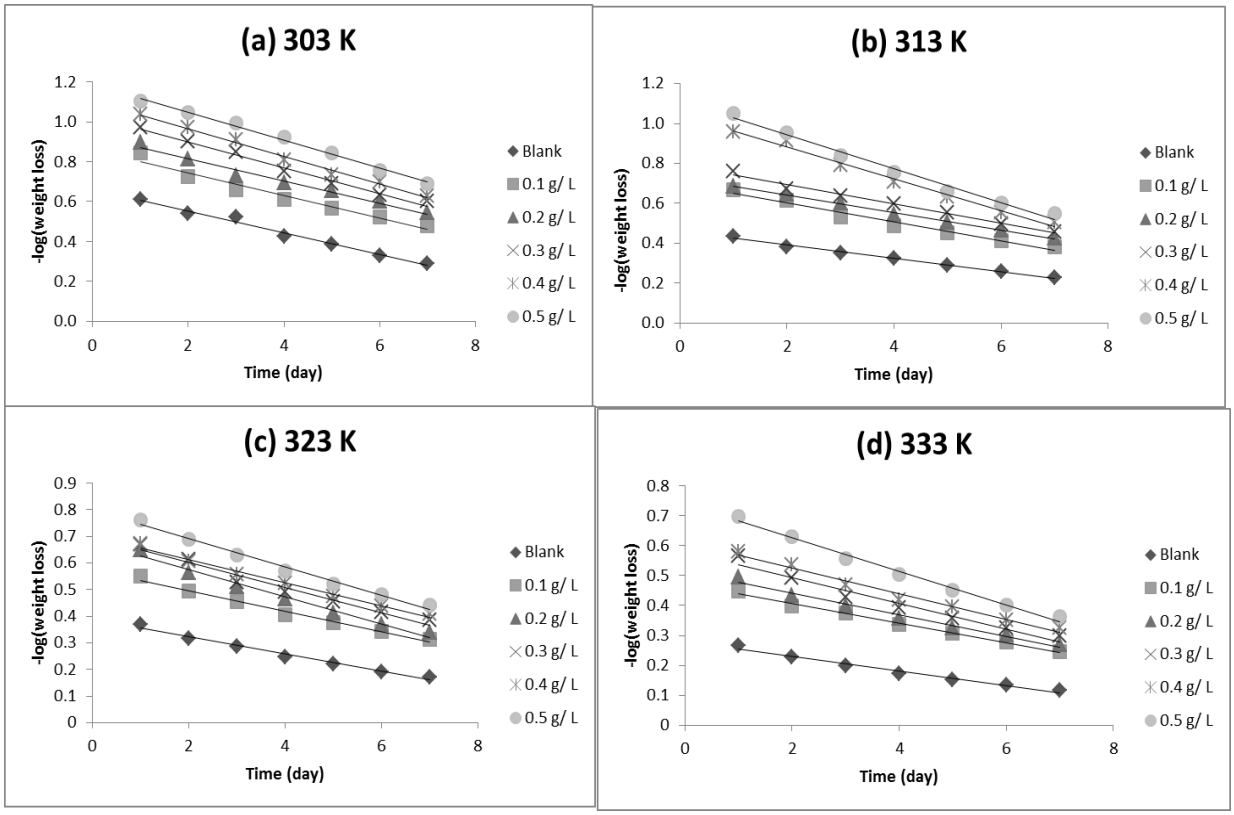

Figure 4. Variation of –log(weight loss) with Time for the Corrosion of Mild Steel in 0.1 M H_3PO_4 Containing Various Concentrations of ACA at 303, 313, 323 and 333 K

Table 3. Kinetic Parameters for the Inhibition of the Corrosion of Mild Steel in 0.1 M H_3PO_4 by ACA

Temperature	System	Slope	k_1	$t_{1/2}$ (day)	R^2
303 K	0.05 g/L	0.0436	0.1103	6.00	0.9910
	0.04 g/L	0.0688	0.1452	4.80	0.9438
	0.03 g/L	0.0951	0.2168	3.20	0.9888
	0.02 g/L	0.1433	0.3314	2.10	0.9632
	0.01 g/L	0.1360	0.3534	2.00	0.9260
	Blank	0.1632	0.3682	1.90	0.9412
313 K	0.05 g/L	0.0245	0.0821	8.40	0.9820
	0.04 g/L	0.0533	0.1424	4.90	0.9660
	0.03 g/L	0.0541	0.1500	4.62	0.9162
	0.02 g/L	0.0761	0.1705	4.06	0.9610
	0.01 g/L	0.914	0.2455	2.82	0.9582
	Blank	0.1014	0.2620	2.65	0.9602
323 K	0.05 g/L	0.0283	0.0533	13.00	0.9902
	0.04 g/L	0.0415	0.0816	8.50	0.9740
	0.03 g/L	0.0515	0.1100	6.30	0.9890
	0.02 g/L	0.0564	0.1504	4.60	0.9720
	0.01 g/L	0.0655	0.1610	4.30	0.9534
	Blank	0.0622	0.1522	4.60	0.9408

333 K	0.05 g/L	0.0228	0.0603	11.50	0.9730
	0.04 g/L	0.0342	0.0713	9.72	0.9622
	0.03 g/L	0.0347	0.0749	9.25	0.9650
	0.02 g/L	0.0413	0.0804	8.62	0.9652
	0.01 g/L	0.0614	0.1021	6.79	0.9870
	Blank	0.0475	0.1284	5.40	0.9620

According to Ameh [26], the first order rate constant is related to the half-life ($t_{1/2}$) through Equation 8.

$$t_{1/2} = 0.693 / k_1 \quad 8$$

Hence, calculated values of $t_{1/2}$ are also recorded in Tables 3. We observed that the half-life of the inhibitor at any instance is greater than that of the blank indicating that the inhibitor increases the half-life of mild steel in solution of H_3PO_4.

3.1.4 Effect of Temperature

The effect of temperature on the corrosion of mild steel in 0.1M H_3PO_4 containing various concentrations of ACA was investigated using the Arrhenius equation (Equation 9) where the apparent activation energy (E_a) for the corrosion process in the absence and presence of inhibitor were evaluated and presented in Table 4. The Arrhenius equation is as given:

$$\ln(CR) = \ln A - \frac{E_a}{RT} \quad 9$$

where *CR* is the corrosion rate of mild steel, *A* is the Arrhenius or pre-exponential factor, *R* is the universal gas constant and *T* is the temperature. The plot of log (*CR*) versus *1/T* yielded a linear relationship with R^2 value tending to unity. The linearity of the plot (Figure 5) indicates that the corrosion of mild steel in the presence of ACA is consistent with Arrhenius theory [27]. The calculated values of E_a were lower than 80 kJ/mol which further support the mechanism of physical adsorption [28].

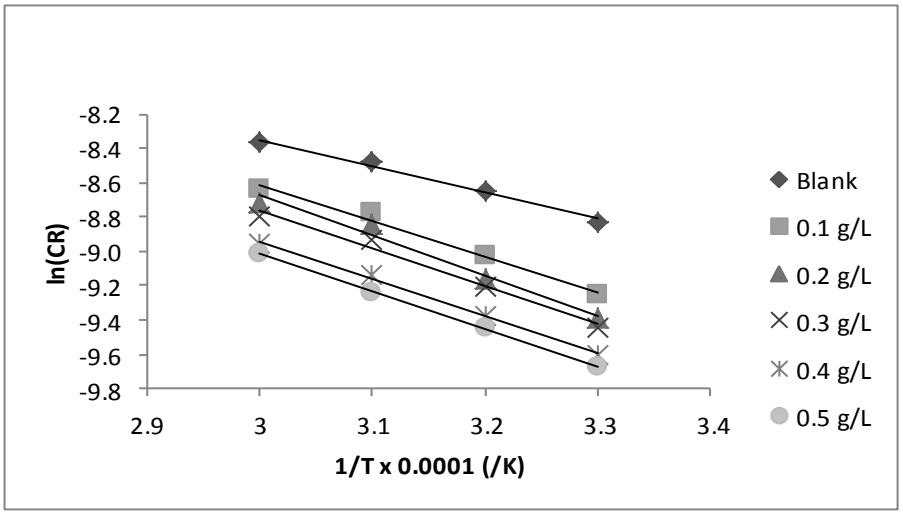

Figure 5. Arrhenius Plots for the Inhibition of the Corrosion of Mild Steel in Solution of H_3PO_4 by ACA

Table 4. Arrhenius Parameters for the Inhibition of the Corrosion of Mild Steel

System	Slope	Intercept	E_a (J/mol)	*A*	R^2
Blank	1.4263	-3.6402	12.76	0.023735	0.9722
0.01 g/L	2.1857	-2.432	17.30	0.000089	0.9800
0.02 g/L	2.2673	-1.5712	18.88	0.000187	0.9512
0.03 g/L	2.3758	-2.2651	16.85	0.000126	0.9545
0.04 g/L	2.2804	-2.3054	16.58	0.000085	0.9884
0.05 g/L	2.1503	-2.2525	16.43	0.0000843	0.9419

3.1.5. Thermodynamic/Adsorption Consideration

The entropy and enthalpy changes for the adsorption of ACA on aluminum surface were calculated using Equation 10 [3].

$$CR = \frac{RT}{Nh}\exp\left(\frac{\Delta S^o}{R}\right)\exp\left(\frac{-\Delta H^o}{RT}\right) \quad 10$$

where R is the gas constant, T is the temperature, N is the Avogadro's number, h is the Plank constant, ΔS^o and ΔH^o are the entropy and enthalpy changes for the adsorption. From the inclusion of logarithm to both sides of Equation (10), Equation (11) was obtained.

$$\log\frac{CR}{T} = \log\frac{R}{Nh} + \frac{\Delta S^o{}_{ads}}{2.303R} - \frac{\Delta H^o{}_{ads}}{2.303RT} \quad 11$$

From Equation 11, a plot of *log (CR/T)* versus *1/T* should be linear and from the slope and intercept of the plot, ΔS^o and ΔH^o can be estimated. Adsorption parameters deduced from the Transition state plot (figure not shown) are recorded in Table 5. From the results obtained, high degrees of linearity were obtained indicating that the adsorption of this inhibitor properly fitted the Transition state model. The values of $\Delta H^o{}_{ads}$, calculated from the slope were found to be negative, indicating that the adsorption is exothermic. Also, the positive values of ΔS^o indicate that the adsorption proceeds with increasing randomness.

Table 5. Thermodynamic Parameters for the Adsorption of Various Concentration of ACA on Mild Steel Surface

System	**Slope**	**Intercept**	$\Delta H^o{}_{ads}$ **(J/mol)**	$\Delta S^o{}_{ads}$ **(J/mol)**	$\mathbf{R^2}$
Blank (0.1 M H_3PO_4)	1.2144	-11.4654	-11.16	136.32	0.9788
0.01 g/L at 303 K	1.7622	-10.8524	-15.80	146.11	0.9824
0.02 g/L at 303 K	2.1820	-9.4137	-17.84	153.58	0.9862
0.03 g/L at 303 K	1.8776	-9.0294	-16.82	149.32	0.9784
0.04 g/L at 303 K	1.8454	-8.0701	-15.46	147.42	0.9848
0.05 g/L at 303 K	1.8565	-8.4238	-15.50	147.45	0.9850

Attempts were made to fit surface coverage data to many adsorption isotherms such as Langmuir, Temkin, Freundlich, Brockris-Swinkle, Frumkim Hill de Boer, Parsons, Dhar-Flory Huggins, Flory Huggins etc. From the isotherm study, Temkin was found to be most suitable (higher regression coefficient) to describe the adsorption behavior of ACA. According to Temkin isotherm model, the concentration of inhibitor C can be related with surface coverage θ by Equation 12.

$$\exp(-2a\theta) = b_{ads}C \quad 12$$

where θ is the surface coverage, C is the inhibitor concentration, 'a' is the molecular interaction parameter and b_{ads} is the equilibrium constant of adsorption process. Rearranging and taking the logarithm of Equation 12, Equation 13 was obtained.

$$\theta = \frac{-2.303}{2a}\log b_{ads} - \frac{2.303}{2a}\log C \quad 13$$

From Equation 13, a plot of θ versus log C should be linear. Adsorption parameters deduced from the plot (Figure 6) are given in Table 6. From the results, it was seen that the slope and R^2 values are very close to unity suggesting that there is a strong adherence of the adsorption of the studied inhibitor to the Temkin model. The applicability of Temkin's adsorption isotherm verifies the assumption of monolayer adsorption on a uniform, homogeneous metal surface with an interaction in the adsorption layer [30].

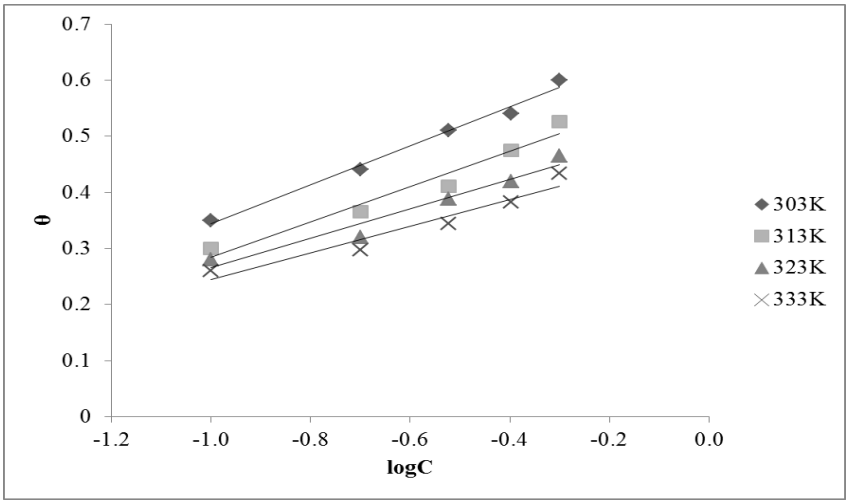

Figure 6. Temkim Plots for the Inhibition of the Corrosion of Mild Steel in Solution of H_3PO_4 by ACA

The free energy for the adsorption (ΔG_{ads}) of ACA on mild steel surface was calculated using the value of the equilibrium constant of adsorption (b_{ads}) obtained from the Temkin adsorption isotherm. According to Eddy *et al.* [11, 28], b_{ads} is related to the equilibrium constant of adsorption according to Equation 14.

$$b_{ads} = \frac{1}{55.5}\exp\left(\frac{\Delta G^{o}_{ads}}{RT}\right) \quad 14$$

The negative values of free energies calculated from Equation 14 (Table 6) are less than the threshold value (-40 kJ mol^{-1}) required for chemical adsorption. Generally, ΔG_{ads} values with magnitude much less than 40 kJ mol^{-1} have typically been correlated with the electrostatic interactions between organic molecules and charged metal surface (physisorption), whilst those of magnitude in the order of 40 kJ mol^{-1} and above are associated with charge sharing or transfer from the organic molecules to the metal surface (chemisorption) [28]. Therefore, the adsorption of ACA on mild steel surface is spontaneous and supports the mechanism of physical adsorption.

Table 6. Temkin Adsorption Parameters for the Inhibition of the Corrosion of Mild Steel by ACA

Temperature(K)	Slope	*a*	log *b*	ΔG^0(kJ mol^{-1})	R^2
303	0.9288	3.68	0.0892	-10.85	0.9565
313	0.6005	3.54	0.0933	-11.26	0.9654
323	0.5997	2.86	0.1078	-11.54	0.9290
333	0.5284	3.50	0.0854	-11.72	0.9582

3.2. Theoretical Studies

The obtained experimental results presented in the previous sections indicated that ACA was a good inhibitor for the corrosion of mild steel in acidic medium. However these results are inconclusive in providing information on the microscopic variables of the molecule. Quantum chemical approaches (semi-empirical and ab initio studies) have therefore been used to complement our experimental results. The semi-empirical parameters were used in correlating experimental results with theoretical data while the ab initio parameters were used in projecting the sites for nucleophilic and electrophilic attacks.

3.2.1. Semi Empirical Models

Semi empirical models serve as efficient computational tools that can yield fast quantitative estimates for a number of properties particularly in the relation of large sets of experimental and theoretical data [14]. Quantum chemical properties calculated using semi-empirical methods during the study include frontier molecular orbital energies (i.e. energies of the highest occupied molecular orbital, E_{HOMO} and that of the lowest unoccupied molecular orbital, E_{LUMO}), the energy gap, ΔE (i.e. $E_{LUMO} - E_{HOMO}$), the electronic energy of the molecule (*EE*), the core-core repulsion energy (*CCR*), the dipole moment (μ) and the heat of formation (H_f) [6]. Table 7 presents values (obtained from gaseous and aqueous phase calculations) for the quantum chemical properties of the studied inhibitor and for different Hamiltonians [(modified intermediate neglect of differential overlap MINDO), Austine model 1 (AM 1), Recief model 1 (RM 1), Parametric model 3 (PM 3) and Parametric model 6 (PM 6)]. It is seen from the results that ACA has relatively high HOMO, low energy gap and low dipole moment which explain its high inhibition efficiency from theoretical point of view. The energy of the HOMO (E_{HOMO}) provides in-

formation about the tendency of a molecule to donate electrons while the LUMO is the unoccupied orbital that has the lowest energy and gives information on the regions in a molecule that have the highest tendency to accept electrons from an electron-rich species. The lower the LUMO energy, the easier the acceptance of electrons from metal surface, as the LUMO−HOMO energy gap decreased and the efficiency of inhibitor improved [11]. The difference in the calculated quantum parameters for the various Hamiltonians is justified by the different assumptions that establish the respective model.

Table 7. Calculated Quantum Energies (eV) of the Inhibitor in the Gas and Aqueous Phase

Phase		**PM6**	**PM3**	**AM1**	**RM1**	**MNDO**
Gas phase	*TE*	-5128.93	-4968.76	-5456.08	-5419.85	-5458.04
	EE	-38185.54	-37654.41	-38483.49	-38568.76	-39491.68
	CCR	33056.61	32685.66	33027.49	33148.91	33033.68
	E_{HOMO}	-8.428	-8.821	-8.598	-8.564	-9.044
	E_{LUMO}	-1.689	-1.803	-1.472	-1.391	-1.653
	ΔE	6.739	7.018	7.126	7.173	7.391
Aqueous phase	*TE* (eV)	-5130.37	-4969.61	-5457.089	-5420.94	-5459.06
	EE (eV)	-7378.87	-6847.15	-7676.470	-7761.74	-7684.62
	CCR	2248.50	1877.55	2219.38	2340.80	2225.57
	μ (Debye)	9.241	4.350	6.310	5.906	4.428
	E_{HOMO} (eV)	-8.341	-8.637	-8.520	-8.464	-8.839
	E_{LUMO} (eV)	-1.745	-1.687	-1.465	-1.311	-1.430
	ΔE (eV)	6.596	6.95	7.055	7.153	7.409

3.2.2. Density Functional Theory (DFT)

In corrosion study, DFT has proven to be powerfully useful for the prediction of the sites for electrophilic and nucleophilic attacks [10, 31]. The molecular properties that were computed using MP2 and B3LYP-6-31G** models include electronegativity, global hardness and softness, electron affinity, ionization potential etc. Ionization potential (IP) and the electron affinity (EA) are defined using the finite difference approximation according to Equations 15 and 16.

$$IP = E_{(N-1)} - E_{(N)} \quad (15)$$

$$EA = E_{(N)} - E_{(N+1)} \quad (16)$$

where $E_{(N-1)}$, $E_{(N)}$ and $E_{(N+1)}$ are the ground state energies of the system with N-1, N and N+1 electrons, respectively. Values of IE and EA calculated from Equations 15 and 16 are presented in Table 8. The results indicate that IP correlated strongly with the E_{HOMO} and EA also correlated strongly with E_{LUMO} indicating that the IE is related to E_{HOMO} while EA is related to E_{LUMO}.

Global hardness (η) measures the resistance of an atom to a charge transfer [32] and it is estimated using Equation 17.

$$\eta = \delta^2 TE/\delta N^2)_{V(r)} = \tfrac{1}{2}(\delta\Upsilon/\delta N)_{V(r)} \quad (17)$$

where Υ is the chemical potential of the electrons, TE is the total energy of the electrons, N is the number of electrons and V(r) is the external potential of the system. Using the finite difference approximation, the global harness and softness (S = 1/η) were calculated as follows [6].

$$\eta = [(E_{(N-1)} - E_{(N)}) - (E_{(N)} - E_{(N+1)})] \quad (18)$$

$$S = 1/[(E_{(N-1)} - E_{(N)}) - (E_{(N)} - E_{(N+1)})] \quad (19)$$

The values of η and S calculated from Equations 18 and 19, respectively, are also presented in Table 8. The fraction of electron transferred, δ can be calculated using Equation 20 [14].

$$\delta = (\chi_{Fe} - \chi_{inh})/2(\eta_{Fe} + \eta_{inh}) \quad (20)$$

where χ_{Fe} and χ_{inh} are the electronegativities of Fe and the inhibitor respectively and can be evaluated as χ = (IP + EA)/2. η_{Fe} and η_{inh} are the global hardness of Fe and the inhibitor, respectively (calculated using Equation 18). The theoretical values of χ_{Fe} = 7ev and η_{Fe} = 0 were used for the computation of δ values for the various Hamiltonians. The calculated values of δ are presented in Table 8. The results indicate that δ values correlate strongly with experimental inhibition efficiencies.

Table 8. Some Gas Phase DFT Parameters for ACA

Model	E_N (eV)	E_{N-1} (eV)	E_{N+1} (eV)	IE (eV)	EA (eV)	χ (eV)	S(/eV)	η (eV)	δ
PM6	-5128.93	-5122.25	-5132.09	6.68	3.16	4.92	0.28	3.52	0.2955
PM3	-4968.76	-4961.84	-4971.87	6.92	3.11	5.01	0.26	3.81	0.2605
AM1	-5456.08	-5448.86	-5458.73	7.22	2.65	4.94	0.22	4.58	0.2255
RM1	-5419.85	-5412.60	-5422.66	7.25	2.81	5.03	0.23	4.44	0.2221
MNDO	-5458.04	-5450.77	-5461.21	7.27	3.17	5.22	0.24	4.11	0.2166

3.2.3. Mulliken Atomic Charges and Fukui Functions

The use of Mulliken population analysis to estimate the adsorption centers of inhibitors has been widely reported and it is mostly used for the calculation of the charge distribution over the whole skeleton of the molecule [31].The Fukui indices for the studied inhibitor was calculated and analyzed along with the distribution of charges in order to have wider knowledge about the local reactivity of ACA. According to Eddy [6], the Fukui indices permit the distinction of each part of a molecule on the basis of its chemical behaviour due to different substituent functional groups. When the Fukui functions are calculated, the sites for electrophilic (f^-) and nucleophilic (f^+) attacks can be accessed assuming that they are controlled by the highest value of f^+ and f^-, respectively. The Mulliken charge distributions of the studied compound together with the calculated Fukui indices for Ab initio, MP2 and DFT level of theories using STO3G basic set for ACA are presented in Tables 9 to 11.From the results obtained, it can be deduced that, the likely sites in the studied inhibitor for electrophilic attack are in N (20), O (12) and O (14). Hence it can be proposed that the areas of N and O atoms are the most possible sites of bonding iron surface by donating electrons to the iron surface.

Table 9. Ab initio (STO3G basic set) Milliken Charges and Fukui Function for ACA

Atom (NO)	q_N	q_{N-1}	q_{N+1}	$f_x^+ \mid e \mid$	$f_x^- \mid e \mid$
N(1)	-0.2723	0.4557	-0.2920	-0.0197	-0.7280
C(2)	0.0894	0.9080	-0.0191	-0.1086	-0.8186
C(3)	-0.0967	0.7295	-0.1329	-0.0361	-0.8263
C(4)	0.1778	1.0187	0.0750	-0.1028	-0.8409
C(5)	-0.0590	1.1188	-0.0445	0.0145	-1.1779
C(6)	0.1304	0.9045	0.0947	-0.0358	-0.7740
C(7)	0.0648	1.2770	0.0475	-0.0173	-1.2122
C(8)	0.0958	1.7602	0.0546	-0.0413	-1.6644
C(9)	0.0604	1.4355	0.0388	-0.0215	-1.3751
C(10)	0.1149	1.2348	0.1078	-0.0072	-1.1198
C(11)	0.3111	-1.0898	0.2857	-0.0255	1.4009
O(12)	-0.2683	-1.3863	-0.3476	-0.0793	1.1180
O(13)	-0.3101	-1.2717	-0.3601	-0.0500	0.9616
O(14)	-0.2720	-0.6102	-0.4069	-0.1349	0.3382
F(15)	-0.1201	-0.0785	-0.1454	-0.0252	-0.0416
F(16)	-0.1250	-0.2928	-0.1576	-0.0327	0.1679
N(17)	-0.3038	0.5784	-0.3079	-0.0042	-0.8822
C(18)	-0.0134	-0.2227	-0.0133	0.0001	0.2093
C(19)	0.0569	-1.1971	0.0568	-0.0001	1.2540
N(20)	-0.3444	-1.8323	-0.3495	-0.0051	1.4879
C(21)	0.0576	-1.0500	0.0573	-0.0003	1.1076
C(22)	-0.0148	-0.4699	-0.0140	0.0007	0.4551
C(23)	-0.1779	-1.0542	-0.1778	0.0001	0.8763
C(24)	-0.1780	-1.1424	-0.1778	0.0002	0.9643
C(25)	0.0361	0.4726	0.0457	0.0096	-0.4365

C(26)	-0.1274	-0.4934	-0.1420	-0.0146	0.3660
C(27)	-0.1335	-0.5667	-0.1403	-0.0068	0.4332
N(28)	-0.4292	0.1966	-0.4376	-0.0084	-0.6258

$q_{(N+1)}$, $q_{(N)}$ and $q_{(N-1)}$ are the Milliken charge of the atom with N+1, N and N-1 electrons

Table 10. MP2 (STO3G basic set) Milliken Charges and Fukui Function for ACA

Atom (NO)	q_N	q_{N-1}	q_{N+1}	$f_x^+ \mid e \mid$	$f_x^- \mid e \mid$
N(1)	-0.2641	-0.2329	-0.2812	-0.0172	-0.0312
C(2)	0.0873	0.1530	0.0133	-0.0740	-0.0658
C(3)	-0.0704	-0.0687	-0.0595	0.0109	-0.0018
C(4)	0.1372	0.1174	-0.0863	-0.2235	0.0198
C(5)	-0.0418	0.0124	-0.0503	-0.0085	-0.0542
C(6)	0.1181	0.0861	0.0656	-0.0524	0.0320
C(7)	0.0308	0.0655	0.0376	0.0067	-0.0347
C(8)	0.0889	0.0768	0.0628	-0.0261	0.0121
C(9)	0.0261	0.0616	0.0365	0.0105	-0.0356
C(10)	0.1027	0.0958	0.0662	-0.0365	0.0068
C(11)	0.2331	0.3312	0.1596	-0.0735	-0.0981
O(12)	-0.2239	0.0564	-0.1713	0.0526	-0.2803
O(13)	-0.2410	-0.1585	-0.2806	-0.0397	-0.0825
O(14)	-0.2364	-0.1150	-0.3539	-0.1175	-0.1214
F(15)	-0.0978	-0.0753	-0.1115	-0.0137	-0.0225
F(16)	-0.1019	-0.0706	-0.1221	-0.0202	-0.0314
N(17)	-0.2914	-0.2926	-0.2968	-0.0054	0.0013
C(18)	0.0216	0.0201	0.0193	-0.0023	0.0015
C(19)	0.0599	0.0605	0.0589	-0.0010	-0.0005
N(20)	-0.2880	-0.2843	-0.2936	-0.0055	-0.0037
C(21)	0.0603	0.0609	0.0592	-0.0011	-0.0007
C(22)	0.0204	0.0186	0.0187	-0.0017	0.0018
C(23)	-0.1002	-0.0998	-0.1005	-0.0004	-0.0003
C(24)	-0.0999	-0.0997	-0.1002	-0.0002	-0.0002
C(25)	0.0379	0.0295	0.0413	0.0034	0.0084
C(26)	-0.0761	-0.0600	-0.0936	-0.0175	-0.0161
C(27)	-0.0865	-0.0792	-0.0997	-0.0132	-0.0073
N(28)	-0.3705	-0.3772	-0.3905	-0.0200	0.0067

$q_{(N+1)}$, $q_{(N)}$ and $q_{(N-1)}$are the Milliken charge of the atom with N+1, N and N-1 electrons

Table 11. DFT (STO3G basic set) Milliken Charges and Fukui Function for ACA

Atom (NO)	q_N	q_{N-1}	q_{N+1}	$f_x^+ \mid e$	$f_x^- \mid e$
N(1)	0.0831	-0.0900	0.4039	0.3208	0.1732
C(2)	0.8782	0.9195	2.0178	1.1396	-0.0413
C(3)	0.6254	1.4757	3.1207	2.4952	-0.8503
C(4)	0.8307	1.7538	3.1590	2.3283	-0.9231
C(5)	0.7292	2.7548	2.1952	1.4660	-2.0256
C(6)	0.6875	3.0561	1.9655	1.2779	-2.3686
C(7)	0.6202	3.5302	2.6824	2.0622	-2.9100
C(8)	-0.0715	3.8380	3.0748	3.1464	-3.9095
C(9)	0.4317	2.8041	2.5316	2.0999	-2.3724
C(10)	0.4250	2.3909	1.9975	1.5725	-1.9659
C(11)	0.0615	-3.5498	2.4548	2.3933	3.6113
O(12)	-1.2544	-1.9907	-1.5755	-0.3211	0.7363
O(13)	-0.9114	-1.9962	-1.3721	-0.4606	1.0847
O(14)	0.8861	-1.6724	4.4608	3.5747	2.5585
F(15)	-0.3346	-0.7080	0.2295	0.5641	0.3734
F(16)	-0.2806	3.4958	-0.2947	-0.0141	-3.7763
N(17)	-0.7109	4.0965	0.7902	1.5011	-4.8075
C(18)	-0.7452	1.2857	-0.4128	0.3324	-2.0309
C(19)	-1.3268	0.8912	-3.6640	-2.3371	-2.2180
N(20)	-0.8720	-1.0243	-2.9937	-2.1217	0.1523
C(21)	-0.1232	0.1331	-3.9640	-3.8408	-0.2562
C(22)	-0.4531	1.4719	-1.5277	-1.0746	-1.9249
C(23)	-0.6552	-2.5346	-3.9984	-3.3432	1.8793
C(24)	-1.3639	-0.6474	-3.9813	-2.6174	-0.7165
C(25)	0.5879	-2.8644	0.7581	0.1703	3.4523
C(26)	-0.5901	-3.9708	-0.4443	0.1458	3.3808
C(27)	-0.6874	-3.9952	-0.5721	0.1153	3.3078
N(28)	0.5560	-0.6646	-0.6800	-1.2359	1.2206

$q_{(N+1)}$, $q_{(N)}$ and $q_{(N-1)}$are the Milliken charge of the atom with N+1, N and N-1 electrons

Figure 7 shows the HOMO and LUMO diagram of the studied inhibitor when it is not adsorbed and when it is adsorbed on the possible sites. The figure generally indicates that the process favours the adsorption of the inhibitor at the sites revealed.

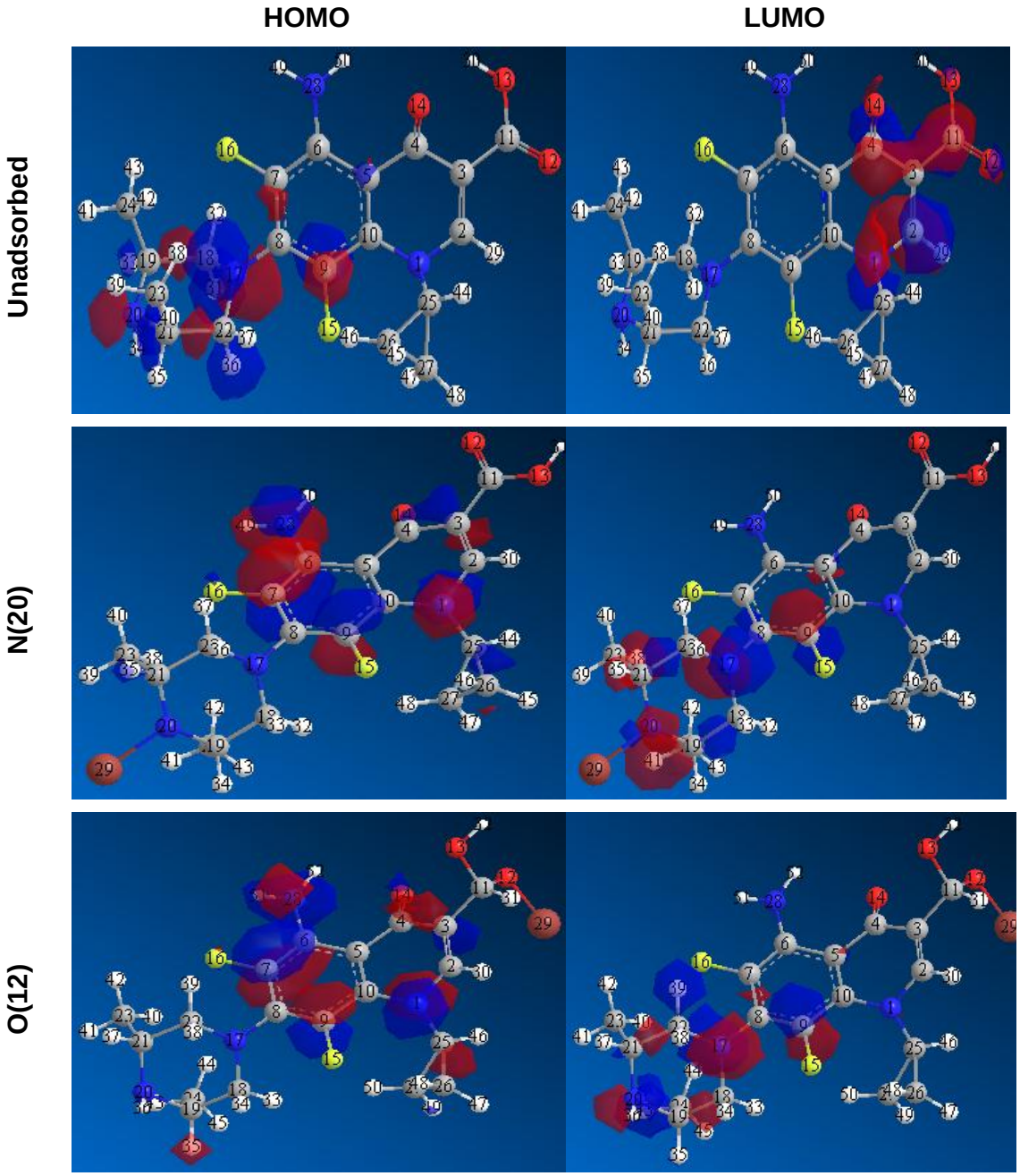

Figure 7. HOMO and LUMO Diagram of ACA Before and After Adsorption on Fe surface

4. Conclusions

The following conclusions can be drawn from this study:

1. ACA acted as a good inhibitor in 0.1 M H_3PO_4 for mild steel corrosion. However, their inhibition efficiencies was found to be effectively enhanced by synergistic combination of KCl, KI and KBr.

2. The blockage of the active sites on the surface of metal through adsorption might be the reason of increased resistance of mild steel against corrosion.

3. The adsorption of the inhibitor on mild steel surface is exothermic (values of ΔH_{ads} were negative) spontaneous (values of ΔG_{ads} were negative) and supports the Temkin adsorption model.

4. The corrosion of mild steel in H_3PO_4 containing various concentrations of ACA follows a first order reaction

5. DFT and quantum chemical studies can adequately be used to study the inhibition potentials of ACA for mild steel corrosion in H_3PO_4 solutions.

6. From the Fukui function calculations, it is indicative that the likely site for electrophilic attack on the studied carboxylic acid is at the N (20), O (12) and O (14).

REFERENCES

[1] Herrag L., Elkadir S., Hammouti B, Aouniti A., 2008. Pyrazole derivatives as corrosion Inhibitors for steel in hydrochloric acid. Port. Electrochim. Acta, 26, 211-220.

[2] Siddiqi W.A., Chaubey V.M., 2008. Corrosion inhibition efficiency of 3- hydroxy-2-methylquinazoline-4-one on mild steel in 1 M H_2SO_4 and 1 M HCl acid at different temperatures. Port. Electrochim. Acta, 26, 221-233.

[3] Ameh P.O., Eddy N.O., 2014. Characterization of *Acacia Sieberiana* (AS) gum and their corrosion inhibition potentials for zinc in sulphuric acid medium, Int J. Novel Res in Phys Chem & Maths., 1(1), 25-36.

[4] Khaled K.F., 2008. Molecular simulation, quantum chemical calculations and electrochemical studies for inhibition of mild steel by triazoles, Electrochim. Acta, 53, 3484–3492.

[5] El Ashry H.E., El Nemr A., Esawy S.A., Ragab S., 2006. Corrosion inhibitors part IV: Quantum chemical studies on the corrosion inhibition of steel in acidic medium by some aniline derivatives. J. Phys Chem., 1, 41-55.

[6] Eddy N.O., 2010. Theoretical study on some amino acids and their potential activity as corrosion inhibitors for mild steel in HCl. Mol. Simul., 35(5), 354-363.

[7] Eddy N.O., Odiongenyi A.O., 2008. Effect of flouro and chloro substituents on inhibition efficiency of quinoliine: Kinetics, thermodynamics and adsorption consideration. J. Phys Chem., 5, 1-9.

[8] El-Subruiti, G. M., Ahmed, A. M., 2002. Kinetic study of corrosion of copper in phosphoric acid tert-Butanol electropolishing mixtures. Port. Electrochim. Acta, 20, 151-166.

[9] Sathiya bama J., Rajendran S., Selvi J.A., Jeyasundari J., 2009. Fluorescein as corrosion inhibitor for carbon steel in well water. Bulgarian Chem. Comm., 41(4), 374-381.

[10] Wang H., Wang X., Wang H., Wang L., Liu A., 2007. DFT study of new bipyrazole derivatives and their potential activity as corrosion inhibitors. J. Mol. Model., 13, 147-153.

[11] Eddy N.O., Ameh P.O., Odey D., Odiongenyi A., 2014. Adsorption and chemical studies on the inhibition of the corrosion of aluminium in hydrochloric acid by *Commiphora africana* gum. Int. J. Chem. Mater. Environ. Res., 1(1), 16-28.

[12] Kraka E., Cremer D., 2000. Computer design of anticancer drugs. J. Am. Chem. Soc., 122, 8245-8264.

[13] Domenicano A., Hargittai I., 1992. Accurate molecular structures, their determination and importance, Oxford University Press, New York.

[14] Eddy N.O., Ibok U.J., Ebenso E.E., Ahmed El Nemr, El Sayed H., El Ashry, 2009. Quantum chemical study of the inhibition of the corrosion of mild steel in H_2SO_4 by some antibiotics. J. Mol. Model., 15(9), 1085-1092.

[15] Arslan T., Kandemirli F., Ebenso E.E., Love I., Alemu, H., 2009. Quantum chemical studies on the corrosion inhibition of some sulphonamides on mild steel in acidic medium. Corros. Sci., 51, 35-47.

[16] Khaled K.F., 2006. Experimental and theoretical study for corrosion inhibition of mild steel in hydrochloric acid solution by some new hydrazine carbodithioic acid derivatives. Appl. Surf. Sci., 252, 4120-4128.

[17] Karelson M., Lobanov V., 1996. Quantum chemical descriptors in QSAR/QSPR studies. Chem. Rev., 96, 1027-1043.

[18] Yurt A., Bereket G., Rivrak A., Balaban A., Erk B., 2005. Effect of Schiff bases containing pyridyl group as corrosion inhibitors for low carbon steel in 0.1M HCl. J. Appl. Electrochem., 35**,** 1025-1032.

[19] Ameh P.O., Magaji L., Salihu T., 2012. Corrosion inhibition and adsorption behaviour for mild steel by *Ficus glumosa* gum in H_2SO_4 solution. Afri. J. Pure Appl. Chem., 6(7), 100-106.

[20] Martinez S., 2002. Inhibitory mechanism of mimosa tannin using molecular modelling and substitutional adsorption isotherms. Mater. Chem. Phys., 77, 97-102.

[21] Abiola O., Okafor N., Ebenso E., Nwinuka N., 2007. Eco-friendly corrosion inhibitors: Inhibitive actions of Delonis regia extract for the corrosion of mild steel in acidic medium. Anti-Corros. Methods Mater., 54, 219-224.

[22] Ameer M.A., Khamis E., Al-Sanani G., 2000. Adsorption studies of the effect of thiosemicarbazides on the corrosion of steel in phosphoric acid. Adsorpt. Sci. Tech., 18, 177-194.

[23] Ameh P.O., Odiongenyi A.O., Eddy N.O., 2012. Joint effect of *Anogessius Leocarpus* gum (AL Gum) exudate and halide ions on the corrosion of mild steel in 0.1 M H_3PO_4. Port. Electrochim. Acta, 30(4), 235-245.

[24] Ebenso E.E., 2003. Synergistic effect of halide ions on the corrosion inhibition of mild steel in H_2SO_4 using 2-acetylphenothiazine. Mater. Chem & Phys., 79, 58-70.

[25] Umoren S.A., Ebenso E.E., 2008. Studies of anti-corrosive effect of Raphia hiikeri exudates gum-halide mixtures for aluminium corrosion in acidic medium. Pigment and Resin Technol., 37(3), 173-182.

[26] Ameh P.O., 2014. Physicochemical characterization and inhibitive performance evaluation of *Commiphora kestingii* gum exudate in acidic medium. Int J. Phys. Sci., 9(8), 184-198.

[27] Oguzie E.E., Li Y., Wang F.H., 2007. Corrosion inhibition and adsorption behaviour of methionine on mild steel in sulphuric acid and synergistic effect of iodide ions. J. Coll. Interf. Sci., 310, 90-98.

[28] Eddy N.O., Awe F.E., Siaka, A.A., Magaji L., Ebenso E.E., 2011. Chemical information from GC-MS studies of ethanol extract of *Andrographis Paniculata* and their corrosion inhibition potentials on mild steel in HCl solution. Int. J. Electrochem. Sci, 6, 4316-4328.

[29] Ashassi-Sorkhabi H., Shaabani B., Seifzadeh D., 2005. Effect of some pyrimidinic Schiff bases on the corrosion of mild steel in hydrochloric acid solution. Electrochim Acta, 50, 3446-3452.

[30] Herle R., Shetty P., Shetty S.D., Kini U.A., 2011. Corrosion inhibition of 304 SS in Hydrochloric Acid Solution by N – Furfuryl N'–Phenyl Thiourea. Port. Electrochim. Acta, 29, 69-78.

[31] Fang J., Li J., 2002. Quantum chemistry study on the relationship between molecular structure and corrosion inhibition efficiency of amides. J. Mol. Struct., 593, 179-185.

[32] Lebrini M., Lagrenée M., Vezin H., Gengembre L., Bentiss F., 2005. Electrochemical and quantum chemical studies of new thia-diazole derivatives adsorption on mild steel in normal hydrochloric acid medium. Corros. Sci., 47(2), 485-505.